

# Design Development and Evaluation of a 2-micron Differential Absorption Lidar for CO<sub>2</sub>

Syed Ismail<sup>1</sup>, Grady J. Koch<sup>2</sup>, Tamer F. Refaat<sup>3</sup>, M. Nurul Abedin<sup>2</sup>, Upendra N. Singh<sup>2</sup>, Manuel A. Rubio<sup>2</sup>, Anthony Notari<sup>4</sup>, Terry Mack<sup>5</sup>, Kenneth J. Davis<sup>6</sup>, James Collins<sup>4</sup>, and Charles Miller<sup>7</sup>

<sup>1</sup>NASA Langley Research Center, MS 401A, Hampton, VA  
<sup>1</sup>757-864-2719; [Syed.Ismail-1@nasa.gov](mailto:Syed.Ismail-1@nasa.gov)

<sup>2</sup>NASA Langley Research Center, MS 468, Hampton, VA

<sup>3</sup>Old Dominion University, Norfolk, VA

<sup>4</sup>SSAI, Hampton, VA

<sup>5</sup>Lockheed Martin, Hampton, VA 23666

<sup>6</sup>The Pennsylvania State University, University Park, PA

<sup>7</sup>Jet Propulsion Laboratory, Pasadena, CA

**Abstract**— This paper presents the design, development, and field testing of a high sensitivity ground-based Differential Absorption Lidar (DIAL) system that was developed under the NASA Instrument Incubator Program. The investigation presents a significant advancement towards the development of future CO<sub>2</sub> profiling capability as it incorporates key elements of technologies needed for a future development of global CO<sub>2</sub> measuring systems including: (1) 2- $\mu$ m laser technologies that have been developed under a number of NASA programs including the Laser Risk Reduction Program (LRRP) (2) A novel high quantum efficiency (QE), high gain (without excess noise factor), and low noise phototransistor, and (3) Direct detection DIAL system using a large collection area receiver that is insensitive to speckle and coherence length effects from atmospheric turbulence that influences heterodyne detection systems. The objective of the project was a system TRL of 4, and the goal was TRL 5. Development and testing of the laser, new detector, and receiver systems during the project, integration into a complete lidar system into a trailer, field testing of system at West Branch, IA and comparison of the lidar CO<sub>2</sub> measurements with *in situ* sensors advanced the system to a TRL of 5. The system demonstrated high vertical resolution CO<sub>2</sub> profiling capability within the boundary layer and column measurements to long ranges. This is the first direct detection demonstration of a 2-micron CO<sub>2</sub> DIAL high vertical resolution capability from instrument concept to field demonstration.

## I. INTRODUCTION

The atmospheric burden of CO<sub>2</sub> is increasing in response to widespread anthropogenic combustion of fossil fuels. Roughly half of the emitted CO<sub>2</sub> is absorbed by the Earth's oceans and terrestrial ecosystems [1]. This uptake [2] varies annually from 1 to 6 PgC yr<sup>-1</sup>. Understanding source/sink processes and the geographic patterns of carbon fluxes are primary goals of carbon cycle science. Uncertainty in predictions of the carbon cycle is one of the leading sources of uncertainty in projections of future climate [3]. A DIAL system operating in the 2.05-micron band of CO<sub>2</sub> was developed for profiling CO<sub>2</sub> in the low-to-

mid troposphere. There are several advantages of this system over passive remote sensing systems including day/night operation, reduction or elimination of interference from clouds and aerosols, and direct and straight forward inversion that leads to better quality data and faster retrievals with few assumptions. A ground-based lidar profiling system with ability to delineate atmospheric boundary layer (ABL) CO<sub>2</sub> from the free tropospheric CO<sub>2</sub> is needed that can operate during day or night. CO<sub>2</sub> distributions in the troposphere are linked to transport and dynamical processes in the atmosphere and are associated with near-surface sources and sinks. Annually averaged, inter-hemispheric, and continental to marine boundary layer CO<sub>2</sub> mixing ratio differences are on the order of 1 to 3 ppm [4]. Thus 0.2 ppm has long been a benchmark for required instrumental precision. Achieving this level of precision is difficult with remote sensors. Much larger mixing ratio differences emerge, however, at smaller spatial and temporal scales. In many instances exchange of ABL CO<sub>2</sub> with the free troposphere takes place through convective activity and passage of weather fronts. Hurwitz et al. [5], describe several synoptic passages and document 10 to 20 ppm mixing ratio changes that result from frontal passages. Thouret et al. [6], have shown that there is a high probability of observing more than one layered structure above the boundary layer at any time. Airborne sampling shows that the majority of the vertical structures in CO<sub>2</sub> mixing ratios are found within the lowest 5 km of the troposphere [4]. Thus, the goal of this DIAL system development was: 0.5% (1.5 ppm) precision for vertical differences in the 30 minute mean mixing ratio resolved every 1 km from 0.5 to 5 km above ground.

In this paper the objectives for the development of the DIAL system are presented followed by descriptions of laser, detector, receiver sub-systems, and integration and field testing of the DIAL system.

## II. TECHNOLOGY DEVELOPMENT OBJECTIVES

This investigation presents a significant advancement towards the development of CO<sub>2</sub> profiling system as it incorporates key elements of technologies needed for a future global CO<sub>2</sub> system. The DIAL system incorporates a high pulse energy, tunable, wavelength-stabilized, and pulsed laser that operates over a pre-selected temperature insensitive strong CO<sub>2</sub> absorption line in the 2.05- $\mu$ m band. The Ho:Tm:LuLF tunable laser is configured to operate at the 2053.204 nm R22 CO<sub>2</sub> line. The system incorporates a newly developed low noise and high gain InGaAsSb/AlGaAsSb (AstroPower) infrared heterojunction phototransistor (HPT) with a 200  $\mu$ m sensitive area diameter. The system was operated in the direct detection mode by taking advantage of a large 16" diameter telescope, which increases the photons collection at the detector by a factor of 16 over our previous system [7] in order to make CO<sub>2</sub> measurements above the boundary layer. Direct detection DIAL system is relatively insensitive to speckle and coherence length effects from atmospheric turbulence that influence heterodyne detection systems. There was no commercially available detector to meet the system objectives at the start of the program.

When the program was initiated in Oct. 2005, previous development in laser technology for building a CO<sub>2</sub> DIAL transmitter and the preliminary lidar proof-of-concept experiment represented a technology readiness level (TRL) of 4. The InGaAsSb/AlGaAsSb phototransistors were characterized in a laboratory environment but not demonstrated in a lidar instrument, represented a TRL of 3. The input system was at a TRL of 3. The objective of the project was achieving a TRL of 4, and the Goal was TRL 5.

## III. LASER DEVELOPMENT AND TESTING

Solid-state lasers based on holmium operating in the 2.05- $\mu$ m region offer several advantages as a transmitter for DIAL measurements of CO<sub>2</sub>: (1) they are tunable in a spectral region containing strong CO<sub>2</sub> absorption lines that are suitable for high sensitivity CO<sub>2</sub> measurements; (2) the absorption lines in this region are relatively temperature insensitive and provide optimum absorption cross-section profiles for tropospheric measurements [8]; (3) there has been considerable development in this laser technology for application in coherent lidar measurements of wind and high energy pulsed diode-pumped Ho:Tm:YLF lasers have been demonstrated [9,10]; and (4) the 2- $\mu$ m wavelength offers a high level of eye safety—a maximum permissible exposure of 100 mJ/cm<sup>2</sup> (ANSI, 2000) [11]. Ho:Tm:LuLF was selected due to its higher optical efficiency and availability of tunable lasers for injection seeding. For developing a successful DIAL profiling system, the following laser characteristics are needed:

- Pulsed laser for range resolved profiling
- Double pulsed operation to sample the same air mass by on- and off-laser pulses
- Wavelength stability and spectrally narrow output

- Line-locking with respect to a selected CO<sub>2</sub> line
- Operation on a side of the line for optimum absorption cross-section selection.

Recent improvements in performance of the laser transmitter include double-pulse operation as demonstrated in the past with other DIAL systems. The double-pulse is injection seeded with different on-off wavelength for each pulse of the doublet. The wavelength switching is accomplished by having two injection seed lasers that can be rapidly (in <1  $\mu$ s) switched by an electro-optic device controlled by a simple logic signal. One of the seed lasers is tuned to the CO<sub>2</sub> line and the second is tuned to off line. The on-line laser is referenced to a CO<sub>2</sub> absorption cell at low pressure, and recent work has improved the performance of the wavelength locking to a level within 390 kHz standard deviation over hour-long time periods. This level of stabilization to line center reflects a factor of 10 improvements over our previous implementation, realized by converting to an external frequency modulation technique rather than wavelength dithering of the laser cavity length. The drift of laser is controlled to <1.4 MHz compared to the free running laser that meets the frequency uncertainty of <2 MHz [12]. An option now exists for tuning the on-line laser to the side of the line rather than the center of the line. By using the side of the absorption line, the optical depth of the DIAL measurement can be tailored for optimal performance. The side line reference is made by locking one seed laser onto line center and referencing a second laser to the center-line laser by monitoring the heterodyne beat signal between the two. A feedback loop has been implemented to lock the side-line laser to the center-line laser. A block diagram of the laser system is shown in Fig. 1.

Electronic control holds an offset from center-line locked laser. Offset can be electronically programmed and laboratory tests have assessed quality of offset lock set up to 2.8 GHz (37.3 pm). Atmospheric tests were conducted

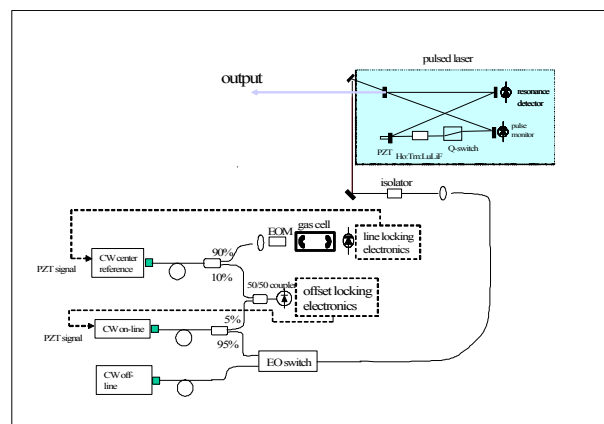


Fig. 1. Block diagram of injection seeded Ho:Tm:LuLF laser; injection seeding setup with line center locked to the CO<sub>2</sub> line, side-line with offset locking with reference to the line and an off-line away from the absorbing line is shown in the lower portion of the figure.

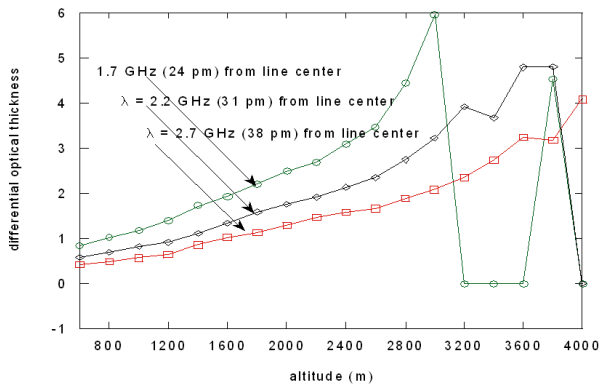


Fig. 2. Atmospheric tests to measure differential optical depths using changing side-line tuning.

in a zenith-pointing mode at NASA Langley during the summer of 2006 using the heterodyne detection system to test the ability to operate in the side-line mode [12]. Fig. 2 shows the results of measurements of differential optical thickness as a function of altitude. The side-line was used as on-line and 3 different side-line positions were used that were offset by 24, 31, and 38 pm from line center. These results indicate ability to operate the laser in the sideline mode to optimize performance by tuning the sideline to desired absorption. More quantitative CO<sub>2</sub> measurements in the atmosphere were made in March, 2007 in the boundary layer using the Ho:Tm:LuLF laser and the existing heterodyne detection system. These DIAL measurements were compared with in situ gas analyzer (LI-COR 6252, [13]) and initial results indicate that the two sensors show the same trend and occurrence of CO<sub>2</sub> perturbations and DIAL data show excellent precision. In the current DIAL system, a side-line wavelength was selected and locked at either 2.15 or 2.80 GHz away from the line center. The unlocked off-line was selected further away (2053.45 nm) from the line center.

#### IV. DETECTOR SYSTEM INTEGRATION AND ATMOSPHERIC TESTS

There were no detectors available commercially that can meet the requirements of the direct detection DIAL system under development. An ideal detector would have high quantum efficiency ( $\sim 70\%$ ), high gain ( $\sim 100$ ) with low noise equivalent power ( $\sim 2E-14$  W/Hz<sup>1/2</sup>) and low excess noise factor of  $< 2.0$ , high bandwidth ( $> 1$  MHz), and fast settling time (1-3 micro seconds to reach 1/100 signal level). A newly developed phototransistor (InGaAsSb/AlGaAsSb; AstroPower) with a 200  $\mu$ m sensitive area diameter was used as the detector of choice [14]. The advantages of the phototransistor are its high gain (up to 3000), lower noise equivalent power (NEP), and higher quantum efficiency ( $\sim 70\%$ ) compared to the traditional extended wavelength PIN photodiodes. These

detectors are sensitive over the wavelength region 1.5 to 2.3 microns with peak performance near 2.05 micron. To capture rapid variations of signals in the lower troposphere, a low gain setting for the phototransistor will be required for the near field and a high gain setting for the far field. Post detector electronics circuit was developed that consists of analog and digital electronic circuit elements. Fig. 3 shows the configuration of the detection system electronics. The features of detection system electronics are:

- Computer controlled detector bias and temperature control electronics.
- Trans-impedance amplifier with dark current compensation.
- Voltage amplifier with offset and gain adjustments.
- A 12-bit waveform digitizer.

However, characterization of these detectors showed lower bandwidth and longer recovery times. The capability of the detector system and its applicability to this program could not be demonstrated at Langley (while the receiver system was still under development). High sensitivity Aerosol Scanning Lidar (REAL: Raman-shifted Eye-safe Aerosol Lidar) system [15] of National Center for Atmospheric Research (NCAR) at Boulder, CO, was used for atmospheric testing by integrating newly developed phototransistors (HPT) into the REAL system. The REAL system has a 16" telescope, two 200-micron APD detector channels, and operates at 1.543-micron wavelength. Atmospheric tests of the detector system were conducted at NCAR initially in June 2006 and later in December 2006 to test the HPT. The 200-micron HPT was used in one of the APD channels and the other APD was used as a reference in the other channel. While the HPT detector is not optimum at 1.543-micron, still, the first atmospheric tests in June 2006 indicated that the HPT has sensitivity to detect atmospheric features (cloud and aerosol layers) to altitudes  $> 5$  km. This was the first time a HPT was used in a lidar system [16]. These tests showed that the HPT could resolve atmospheric features  $\sim 100$  m in size (even for a 3 V high-gain setting at 20 °C).

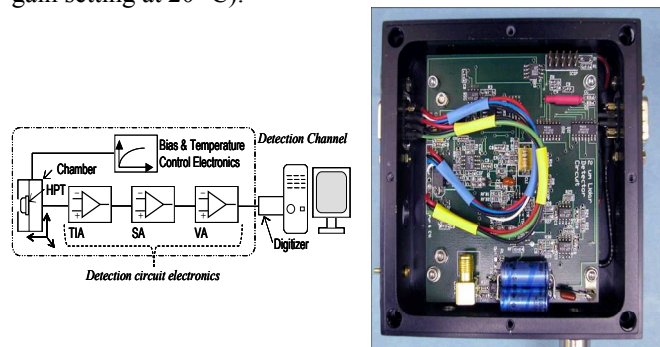


Fig. 3: (a) Schematic of the lidar detection system that consists of the lidar detection channel and the digitizer. The lidar detection channel is formed by the HPT and the detection circuit electronics. The electronics include transimpedance amplifier (TIA), summing amplifier (SA), and voltage Amplifier (VA). (b) Picture of the detection channel electronics after integration discussed in [16].

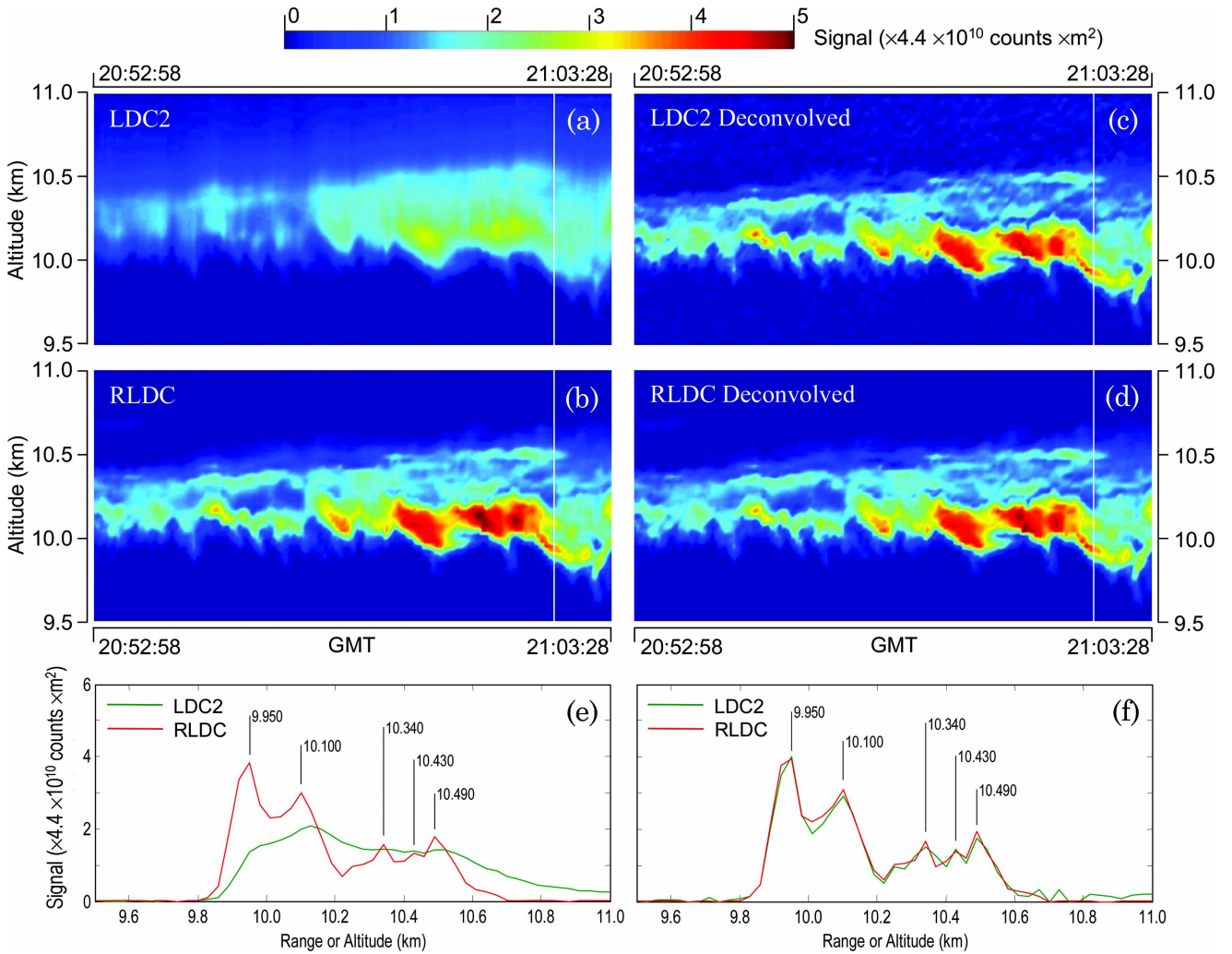


Fig. 4: False color history diagrams of the far-field temporal variation of the return signal before de-convolution (a) for the HPT lidar detection channel and (b) for the REAL APD reference detection channel. The same diagrams are repeated for (c) HPT channel and (d) APD reference channel after de-convolution. The vertical white line selects a sample record shown in (e) and (f), which mark some resolved peaks, down to 60 m, after the de-convolution processing [17].

However, lower bandwidth and slower recovery problems cause systematic effects in data from the HPT system compared to the APD system. To minimize systematic effects due to the bandwidth and slow recovery and to retrieve atmospheric lidar data from the HPT channel further lab characterizations were conducted at NCAR including impulse response tests using a short (0.1  $\mu$ s) pulse laser and dynamic linearity tests using simulated lidar signal profiles [17]. Data from the impulse response tests were used to deconvolve measurements from the HPT channel. An iterative convolution technique was employed that is a modification of an earlier technique [18]. Results of deconvolution using this procedure are shown in Fig. 4 and for both HPT and APD channels.

The deconvolution process eliminated recovery, increased resolution, and minimized phase delay between HPT and APD data channels as shown in Fig. 4. The deconvolution procedure was fast and was implemented for the whole series of measurements with consistent results. Some degradation of signal-to-noise (S/N) in the low S/N regions was observed.

## V. RECEIVER SYSTEM

The optical receiver uses a 16-inch diameter F/2.2 all aluminum telescope to minimize influences of thermal effects. This custom designed telescope was manufactured by Welch Mechanical Design, Baltimore, MD. One of the specifications for this telescope was to have a small (45 micron diameter) focus area (blur spot size). The optical scheme of the receiver is shown in Fig. 5. The incident light is focused by the two mirrors of Cassegrain telescope through the pinhole and coupled into a fiber optic. The receiver optics includes a collimating lens, narrowband interference filter, focusing lenses, and protective window. The optical design includes focusing the optical signal onto the 200- micron diameter detector. The laser beam is transmitted into the atmosphere co-axially after a 20X beam expansion to limit the transmitted field of view to 85 micro-radians. The receiver FOV is set to 350 micro-radians using a pinhole at the focus of the telescope. Light from the telescope focus spot is coupled to the collimating lens of the aft.-optics system by a multimode optical fiber. The

telescope, aft.-optics, detectors, and other components are placed inside an all-Aluminum enclosure box to limit stray light from the laser. This box also provides optical baffling and overall structural support. Besides, the box enclosure could be purged with nitrogen if detector cooling below zero is required. Fig. 6 illustrates the integrated CO<sub>2</sub> DIAL system [19].

After integration, the CO<sub>2</sub> DIAL system was aligned and tested at LaRC. System alignment included adjustment of the distance between the beam expander lenses, tilt adjustment of the beam steering mirrors, locating the telescope focus point and adjustment of the optical fiber to that point. The other side of the optical fiber was also aligned to the collimating lens, while the HPT was aligned to the focusing lens. Auxiliary CW alignment lasers were set for aiding in the alignment procedure. The alignment of the system was challenging! Laser output beam was aligned with the receiver, light collected from the 16" telescope was focused on exactly positioned fiber optic cable at the telescope focus, the fiber optic cable was terminated at the focus spot of the collimating lens, and the detector was positioned at the <200 micron focus spot of the focusing lens. In addition, verification was made using a knife edge optical set-up that the focus spot size at the detector was smaller than 200 microns in size. The alignment procedure was applied only once to conduct a series of measurements and during the field experiment. After this was achieved, detector alignment was repeated only once during a testing sequence. The lidar system parameters are given in Table 1. On February 2008 initial testing of the system resulted in the capture of the first high-resolution atmospheric backscatter signal at 2-μm wavelength.

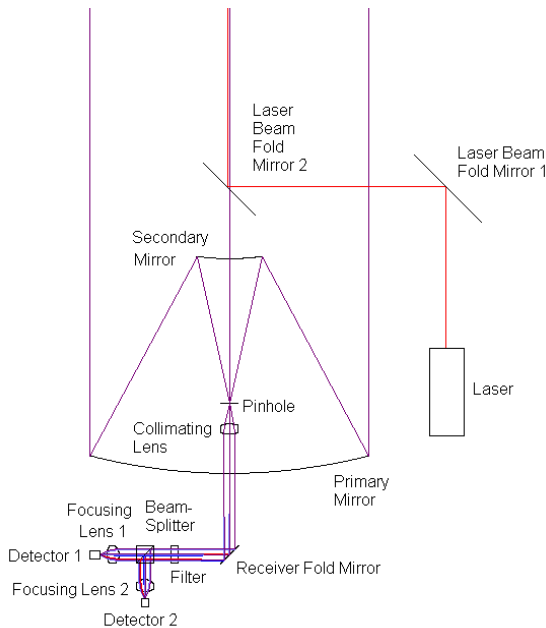


Fig. 5: Schematic diagram of the optical design of the receiver system, including the aluminum telescope and the aft-optics, with two detection channel capability.

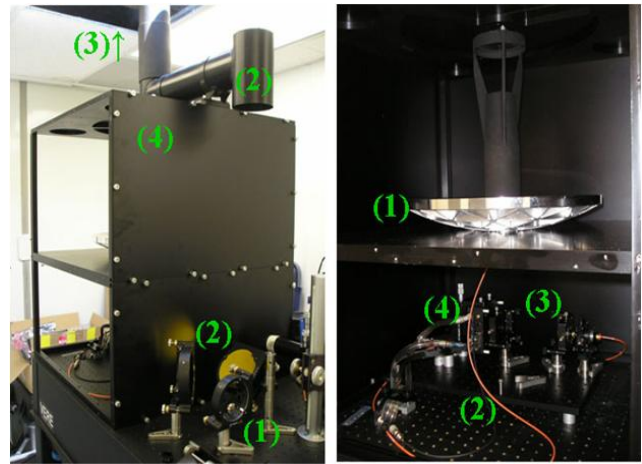


Fig. 6: Pictures of the CO<sub>2</sub> DIAL receiver box (a) beam expander lens (1) and beam steering optics (2) guide the transmitted beam to the atmosphere co-axially with the telescope through top window (3). Receiver enclosure box (4) allows for optics shielding and components environmental control. (b) Receiver system hardware including 16" all aluminum telescope (1), fiber coupled (2) to aft-optics (3) that focuses the radiation onto the detector (4).

TABLE 1  
LIDAR SYSTEM PARAMETERS

Pulse Energy	90 mJ
Pulse width	180 ns
Pulse rep. Rate	5 Hz
Spectrum	Single frequency
On-line wavelength	2053.204 nm
Off-line wavelength	2053.45 nm
Beam quality	<1.3 diff. Limit
Wavelength stability	1.4 MHz
Wavelength accuracy	<0.4 MHz
Detector	InGAS/AIGAS
Quantum efficiency	70%
NEP	5.0E-14 W/sqrt(Hz)
Telescope diameter	16"
Receiver FOV	385 mRadian

## VI. DIAL SYSTEM TESTS AND FIELD MEASUREMENTS

After successful integration on a trailer and ground testing at NASA Langley [19], a field campaign was conducted at West Branch, Iowa, June 20, 2008 to July 8, 2008, in order to further test and validate the CO<sub>2</sub> DIAL system. At this location, three CO<sub>2</sub> *in-situ* sensors were installed and operated by NOAA on the KWKB-TV tower (WBI tower) at 31, 99 and 379 m altitudes. The WBI site has several advantages for the CO<sub>2</sub> DIAL measurements including easy access of *in-situ* sensors data for instrument validation. In addition, complementary NOAA aircraft sampling aided in obtaining CO<sub>2</sub> mixing ratios at higher

altitudes. In this campaign sonde launches were conducted to collect meteorological data twice everyday to minimize the uncertainty in the CO<sub>2</sub> measurements from DIAL.

High resolution spectroscopic measurements were conducted at the Jet Propulsion Laboratory to derive accurate line parameters of the R22 CO<sub>2</sub> line. Details of the data analysis techniques and CO<sub>2</sub> retrieval methodology is given in Tamer et al., 2010 [20].

The DIAL system was operated almost continuously from the morning of July 5<sup>th</sup> till the afternoon of July 6<sup>th</sup>, 2008. Fig. 7 shows the lidar false color diagram for the off-line and side-line range corrected profiles. In the first and last sections (labeled I & IIIB on figure) the side-line was tuned 2.8 GHz off the R22 line center and during the night it was operated at 2.15 GHz. Metrological data were collected twice during the daytime and standard atmospheric models were applied for night time. Initial CO<sub>2</sub> mixing ratio profiles at a range resolution of 30 m were obtained by averaging 300 laser shot pairs and deconvolution of signals with 100 iterations. These data were further averaged to obtain CO<sub>2</sub> profiles at 300 to 450 m range resolutions with 5-points temporal smoothing average. Fig. 7 also shows a comparison of the DIAL with the WBI tower-379 m sensor.

Night measurements indicated lower noise compared to day due to the influence of the day background. Since it is closer to the line peak, operating at 2.15 GHz sideline resulted in better near-field sensitivity but with higher attenuation due to stronger absorption. Tuning further away from the line peak, at 2.80 GHz, allows range extension leading to better far-field sensitivity.

One advantage of the DIAL system is the ability to perform integrated CO<sub>2</sub> column measurements. This is demonstrated using data collected on June 26, 2008. On that day, weather conditions included a continuous, variable altitude cirrus cloud, as indicated in the false color diagrams of Fig. 8. Vertical column integration was performed between the near-field high scattering from the boundary layer and the far-field scattering from the cloud. Thus, the column length was variable ranging in the 4 to 9 km range.

Fig. 8 shows the range corrected lidar signals for the off-line (top) and side-line (bottom) in log scale. Also, shown in the figure are the calculated CO<sub>2</sub> effective average mixing ratio from the column DIAL integration, compared with the mixing ratio of the WBI tower 379 m *in-situ* sensor data. Details of column DIAL measurements are given in Tamer et al., 2010 [yy]. During these measurements, the side-line was tuned to 2.8 GHz. DIAL data analysis included 200shot averages without deconvolution.

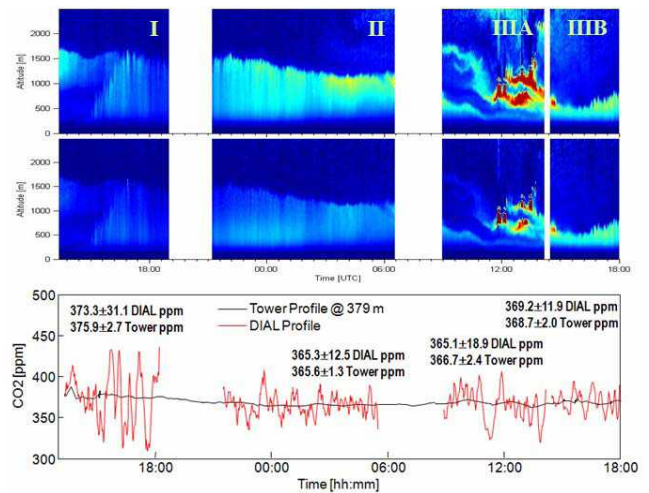


Fig. 7. False color diagrams for the off-line (top) and side-line (middle) of the range corrected signal profiles. The data was collecting from the morning of July 5<sup>th</sup> till the afternoon of July 6<sup>th</sup>, 2008 with 2.80 GHz (sections I and IIIA) and 2.15 (sections II and IIIB) tuning. The calculated CO<sub>2</sub> mixing ratio of the DIAL and 379 m tower sensor are compared in the bottom.

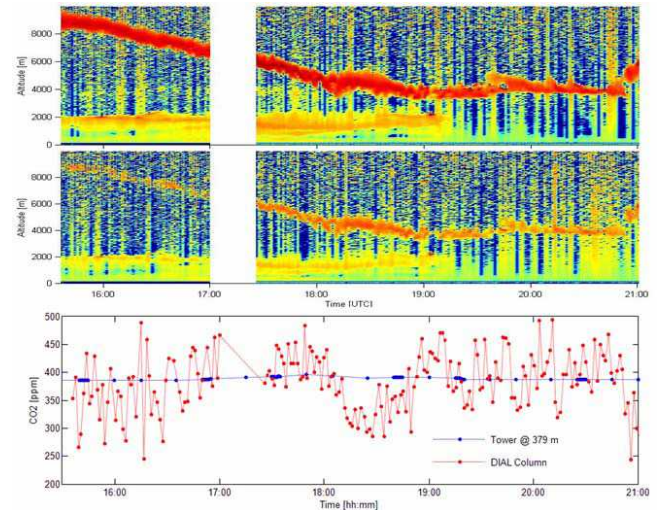


Fig. 8. False color diagrams for the log of the range corrected off-line and side-line profiles (top and middle) from measurements on June 26, 2008. The calculated effective average CO<sub>2</sub> mixing ratio of the DIAL and tower sensor are compared in the bottom.

## VII. SUMMARY AND RECOMMENDATIONS

The 2-micron IIP DIAL program concluded successfully by completing all milestones on time and within cost. The system demonstrated high vertical resolution CO<sub>2</sub> profiling capability within the boundary layer and column measurements to long ranges. There was good agreement between DIAL CO<sub>2</sub> measurements and tower-based *in situ* observations from West Branch, IA. Measurements above the boundary layer were limited due to low aerosol loading in the atmosphere. The Ho:Tm:LuLF laser was operated for the first time on the side of the CO<sub>2</sub> line by off-set locking up to 2.9 GHz..

Precise tuning was demonstrated and wavelength stability were improved by more than an order of magnitude to reduce systematic errors, from these sources, to <0.1%. At the start of the program, no detectors were commercially available that were suitable for the 2-micron DIAL application. InGaAsSb/AlGaAsSb based hetero-junction phototransistor was configured and lidar measurements were made for the first time using a phototransistor as a detector. Iterative deconvolution procedure was used for the first time in lidar to remove detector systematic effects. This is the first direct detection demonstration of a 2-micron CO<sub>2</sub> DIAL profiling capability from instrument concept to field demonstration.

With the development and testing of the laser, new detector, and receiver systems during the project, integration into a complete lidar system into a trailer, field testing of system at West Branch, IA and comparison of the lidar CO<sub>2</sub> measurements with *in situ* sensors (showing good agreement with the *in situ* tower sensors) advanced the system TRL to 5.

There is a critical need to develop a new detector (low noise, high gain APD that is free from systematic effects) to be operated in the 2-micron region for developing future direct detection systems (airborne or space). New detectors development that that have the potential to meet the requirements are HgCdTe, and InGaAs APD's. To enhance the system performance (i.e reduce noise and minimize systematic effects) two steps are recommended: the DIAL system be reconfigured to operate on the CO<sub>2</sub> line at 2.051 micron using the Ho:Tm:YLF laser for enhanced performance (~double laser output power by double pulsing, minimum interference from H<sub>2</sub>O lines, and less sensitivity of CO<sub>2</sub> absorption to atmospheric temperature); and system optimization with custom optics, lower detector temperature operation, improved optical coupling, and elimination of e-m interference that was observed in some signals that (these shots were edited out). A major source of error (noise and bias), during this program, in DIAL measurements of CO<sub>2</sub> was the interference by H<sub>2</sub>O absorption at the R22 line. Non-availability of tunable seed laser source inhibited operation at the preferred R30 line

#### ACKNOWLEDGEMENTS

This work is supported by 2- $\mu$ m CO<sub>2</sub> DIAL IIP Project under NASA's Earth Science Technology Office. The authors would like to thank Dr. Jiron Yu for consultations on laser developments, Bruce Barnes for development of data acquisition software; Yonghoon Choi and Stephanie Vay for providing *in situ* data for comparison with DIAL measurements; and Shane Mayor, Scott Spuler and NCAR management for their support and facilities for conducting detector tests at NCAR, Boulder, CO.

#### REFERENCES

[1] Battle, M. et al., "Global carbon sinks and their variability inferred from atmospheric O<sub>2</sub> and  $\delta^{13}C$ ", *Science*, **287**, 2467-2470, 2000.

[2] Conway, T.J., et al., "Evidence for interannual variability of the carbon cycle from the National Oceanic and Atmospheric Administration/Climate Monitoring and Diagnostics Laboratory Global Air Sampling Network" *J. Geophys. Res.*, **99**, 22831-22855, 1994.

[3] Friedlingstein, P. et al., "Positive feedback between future climate change and the carbon cycle", *Geophys. Res. Lett.*, **28**, 1543-1546, 2001.

[4] Yi, C. et al., "The observed covariance between ecosystem carbon exchange and atmospheric boundary layer dynamics in North Wisconsin", *J. Geophys. Res.*, **109**(D08302): doi10.1029/2003JD004164, 2004.

[5] Hurwitz, M.D. et al., "Advection of carbon dioxide in the presence of storm systems over a northern Wisconsin forest" *J. Atmos. Sci.*, **61**, 607-618. 2004.

[6] Thouret, V. et al., "General characteristics of tropospheric trace constituent layers observed in the MOZAIC program", *J. Geophys. Res.*, **105**, 17,379-17,392, 2000.

[7] Koch, G. J. et al., "Coherent differential absorption lidar measurements of CO<sub>2</sub>", *Appl. Opt.* **43**, 5092-5099, 2004.

[8] Menzies, R.T. and D.M. Tratt, "Differential laser absorption spectrometry for global profiling of tropospheric carbon dioxide: selection of optimum sounding frequencies for high-precision measurements", *Appl. Opt.*, **42**, 6569-6577, 2003.

[9] Singh, U.N., J. Yu, M. Petros, N.P. Barnes, J.A. Williams-Byrd, G.E. Lockhard and E.A. Modlin, "Injection-Seeded, Room-Temperature, Diode-Pumped Ho:Tm:YLF Laser with Output Energy of 600 mJ at 10 Hz", *Advanced Solid-State Laser Conference*, vol. 19 of OSA Trends in Optics and Photonics Series, p. 194, 1998.

[10] Yu, J., A. Braud, and M. Petros, "600mJ, double-pulse 2- $\mu$ m laser", *Opt. Lett.* **28**, 540-542, 2003.

[11] American National Standard (ANSI) Z136.1, 2000.

[12] Grady J. Koch, Jeffrey Y. Beyon, Fabien Gibert, Bruce W. Barnes, Syed Ismail et al., Side-line tunable laser transmitter for differential absorption lidar measurements of CO<sub>2</sub>: design and application to atmospheric measurements, *Applied Optics*, Vol. 47, Issue 7, pp. 944-956, 2008.

[13] Vay, S.A. et al., "Airborne observations of the tropospheric CO<sub>2</sub> distributions and its controlling factors over the South Pacific basin", *J. Geophys. Res.*, **104**, 5663-5676, 1999.

[14] Refaat, T.F. et al., "AlGaAsSb/InGaAsSb phototransistors for 2- $\mu$ m remote sensing applications", *Optical Engineering*, Vol 43, No 7, 1647, 2004.

[15] Mayor, S. and S. Spuler, "Raman-shifted eye-safe aerosol lidar", *Applied Optics*, **43**(19), 3915-3924, 2004.

[16] T. Refaat, S. Ismail, T. Mack, N. Abedin, S. Mayor, S. Spuler, and U Singh, "Infrared Phototransistor Validation for Atmospheric Remote Sensing Application using the Raman-Shifted Eye-Safe Aerosol Lidar (REAL)", *Opt. Eng.* 2007 (in press).

[17] Refaat, T., S. Ismail, N. Abedin, et al., "Lidar Backscatter Signal Recovery from Phototransistor Measurement Effects by Deconvolution" *Appl. Opt.* 2008.

[18] van Cittert, P. "Zum einfluss der spaltbreite auf die intensitätsverteilung in spektallinien", *Z. Phys.* **69**, 298-308, 1931.